EXTENSION OF THE POLAR CORONAL HOLE BOUNDARY INTO INTERPLANETARY SPACE

Richard Woo

Jet Propulsion Laboratory, California Institute of Technology, 4800 Oak Grove Drive, MS 238-725, Pasadena, CA 91109

Shadia Rifai Habbal

Harvard-Smithsonian Center for Astrophysics, 60 Garden Street, Cambridge, MA 02138

Russell A. Howard and Clarence M. Korendyke

Hulburt Center for Space Research, Naval Research Laboratory, Washington DC 20375

Submitted to Astrophysical Journal
April xx, 1998

ABSTRACT

White-light measurements made by the Mk III Mauna Loa K-coronameter and the SOHO LASCO C2 and C3 coronagraphs, extending from 1.15 to 30 Ro, have been combined to show that the boundaries of polar coronal holes, as determined by measurements of path-integrated density, extend approximately radially into interplanetary space. These results are in contrast with the longstanding view that the boundaries of polar coronal holes diverge significantly beyond radial, evolving around the edges of streamers. The combined observations also show that the corona is dominated by raylike structures as small as a few degrees in angular size with respect to Sun center, originating from both coronal holes and quiet Sun regions. This analysis provides further support for results originally derived from radio occultation measurements, namely that, with the exception of the narrowing of streamers into stalks, the coronal density projects itself almost radially from the Sun into the outer corona. It also reinforces the view that the fast solar wind originates from both coronal holes and quiet Sun regions.

1. INTRODUCTION

Knowledge of the distribution of electron density in the solar corona is not only fundamental for understanding the structure of the corona itself (e.g., Saito 1965, Newkirk 1967, Koutchmy 1977), it also provides important clues for the origin and evolution of the solar wind (Munro and Jackson 1977, Lallement et al. 1986, Guhathakurta 1989, Habbal et al. 1997, Woo and Habbal 1997a). The primary sources of information on electron density in the solar corona have been white-light (e.g., van de Hulst 1958, Koutchmy 1977, Guhathakurta and Fisher 1995) and radio occultation measurements (e.g., Bird and Edenhofer 1990). The former are made during solar eclipses and with white-light coronagraphs, while the latter are conducted when spacecraft radio signals or natural radio sources are occulted by the solar corona. Both measurements share a common observable, namely path-integrated electron density. However, despite extensive observations, only recently has an understanding of the relationship between these complementary measurements begun to emerge (Woo 1996a).

By probing the coronal density as a function of latitude starting from the pole, ranging measurements of the outer corona near 20 Ro have shown evidence for a slight increase in density at approximately 30° from the polar axis (Woo and Habbal 1997a). When compared with the corresponding Mk III white-light coronagraph image of the Sun, the increase was found to occur where the line of sight intercepted the radial extension into the corona of the polar coronal hole boundary at the solar surface. In addition, the character of the Doppler scintillation was found to still resemble that of a fast wind. Woo and Habbal (1997a) concluded that the boundary of the polar coronal hole extends almost radially from the solar surface, and that the fast wind originates also from the quiet Sun (regions on the Sun other than coronal holes and active regions).

Another result revealed by radio occultation measurements has been the dominance of raylike structures of a few degrees in angular size in the corona (Woo and Habbal 1997a). The brightest of these are the streamer stalks (Woo et al. 1995a,b) which occupy only a

small volume in interplanetary space (Woo and Habbal 1997a). The remaining raylike structures — often referred to as plumes or polar rays in polar coronal holes — are not limited to polar regions, but also originate from low latitude coronal holes (Woo 1996b) as well as from within the boundaries of coronal streamers as seen projected off the limb in the plane of the sky (Woo and Habbal 1997a).

With white-light observations extending beyond a few solar radii, the expanded capabilities of the Large Angle Spectrograph Coronagraph (LASCO) on board the Solar Heliospheric Observatory (SOHO) (Breuckner et al. 1995) offer an unprecedented opportunity to explore: (1) the extension of the boundaries of polar coronal holes into interplanetary space, and (2) the ubiquity of raylike structures.

2. OBSERVATIONS

Examples of the combination of measurements used in this study are displayed in Figure 1 for 11 August 1997. These consist of soft X-ray images of the Sun obtained by Yohkoh (Tsuneta et al. 1991), Mauna Loa Mk III polarized brightness (pB) measurements (Fisher et al. 1981) of the inner corona out to 2 Ro, and white-light images obtained with the LASCO C2 and C3 coronagraphs (Brueckner et al. 1995) extending from 2 to 30 Ro (Figures 1a-d). Both C2 and C3 are externally occulted coronagraphs. Since the supporting pylon of the occulters is located in the southeast quadrant of the field of view (around position angle 130°) we limit this investigation to the northern hemisphere, i.e., position angles 0–90° and 270–360° (where position angle is measured counterclockwise starting from 0° at the north pole).

Each telescope has its own 1024 x 1024 pixel CCD camera, which records images with a two-pixel spatial resolution of 23" (C2) and 112" (C3) respectively, except near the inner edge of the field of view where vignetting by the external occulter degrades the resolution. A background image was produced from either a week or a month of observations. For each day of observations, a given exposure of the total intensity, including both polarized

and unpolarized components of the C2 and C3 coronagraphs, was corrected for noise and cosmic ray hits. An average image was then made from at least four exposures. The images shown in Figures 1b and 1c were produced by dividing the average by the background, yielding a much higher contrast for the faint structures.

On the other hand, the azimuthal profiles of the total intensities, shown in Figure 1e at altitudes of 2.8 and 3.6 Ro (middle panel) and 5.6 and 7.4 Ro (lower panel), were computed from the corrected average images obtained by subtracting the background image from the average image. The azimuthal profiles of polarized brightness (pB) from the Mauna Loa Mk III coronameter, displayed in the upper panel of Figure 1e at altitudes of 1.15, 1.25, 1.35 and 1.45 Ro, were provided by J. Burkepile.

3. CORONAL HOLE RESULTS

The existence of a ledge or plateau in the azimuthal profile of electron density was first identified in radio occultation measurements (Woo and Habbal 1997a). This plateau started near the radial extension of the coronal hole boundary at the Sun moving towards lower latitudes. The increase in density across that boundary was about a factor of two, We illustrate in the following examples how these ledges appear in the white-light data, and how their detection depends on structures forming the boundaries of coronal holes.

In addition to the example of Figure 1, the analysis presented here is based on observations made during the period of 15 August 1996 to 8 September 1996. Examples from 15 August and 5 September are shown in Figures 2 and 3, respectively. The polar coronal hole boundaries, as projected on the solar disk and best defined by the He I 1083 nm maps of the National Solar Observatory, are superimposed in yellow on the soft X-ray image in Figures 1–4. As viewed on the solar disk, the He I coronal hole boundaries are in general agreement with boundaries identified by the soft X-ray emission. Yellow straight lines have also been drawn in Figures 1–3 to indicate the radial extensions of the

polar coronal hole boundaries starting from the He I boundaries at the limb and extending into the corona. Since the purpose of these lines is to guide the eye, they have been drawn only on those parts of the images where azimuthal variations cannot be discerned. These same boundaries are represented by the red vertical lines on the azimuthal profiles of Figures 1e, 2d, 3d, and 4c.

In the measurements of 11 August 1997 (Figure 1), the narrowing of coronal streamers with increasing altitude in the Mk III images is reflected in the pB profiles above 1.15 Ro as an apparent shift of the coronal hole boundaries towards lower latitudes. This shift is, however, not evident in the higher altitude profiles of C2 and C3. On the contrary, the coronal hole boundary extends approximately radially with increasing heliocentric distance. The coronal hole boundary in the outer corona is especially striking in Figure 1d, which shows the C3 image of polarized intensity with its contrast enhanced in order to highlight the subtle density change across the boundary.

In the azimuthal density profile, the coronal hole boundary may appear as a ledge (extending between the red and green vertical lines in Figures 1e and 2d), as on the NE limb (between 30–60° latitude), or it may mark the beginning of the steepening streamer in cases where the ledge is masked by the steeply rising streamer, as on the NW limb. In the latter cases, the ledge will eventually be revealed at larger heliocentric distances where the steeply rising streamer is narrower. Although the coronal hole boundary appears as a weak feature in the presence of the steeply rising streamer profile, the rise in path-integrated density across the boundary is still about a factor of two, similar to that near the Sun in the Mk III measurements at 1.15 Ro. Starting as a weak feature at the Sun, the coronal hole boundary, therefore, persists as a weak feature as it extends into interplanetary space.

The apparent shift in coronal hole boundary in the Mk III profiles is a consequence of measurement sensitivity diminishing with increasing heliocentric distance. For the C2 and C3 coronagraphs, the detection is hampered at large heliocentric distances for the same reason. However, the detection of the coronal hole boundary also depends on other

factors. The boundary is especially prominent when the density of the quiet Sun is high, as when active regions and/or coronal streamers are present at high latitudes, such as in the example of Figure 1. The measurements of 15 August 1996 (Figure 2) illustrate that the coronal hole boundary is also evident when there is a high-latitude streamer but no active region (NW limb), and when a low-latitude streamer is present (east limb). The corresponding intensity profiles show that, while the ledge of the coronal hole boundary is narrow in the case of the high-latitude streamer (at NW around 50–60° latitude), it is broad for the low-latitude streamer (at NE between 30° to 70° latitude).

The NE limb on 5 September 1996 (Figure 3) is a case in which the coronal hole boundary was not observed in the outer corona. The east limb is relatively free of active regions and high-latitude streamers. However, the most likely reason for the absence of the boundary is the extension of the north polar coronal hole to low latitudes as shown by the Yohkoh soft X-ray measurements in Figure 3a. In this case, contributions from the quiet regions in front or behind the plane of the sky enhance the observed intensities and can mask the coronal hole boundary signature or ledge. The latitude of the coronal hole boundary is, therefore, another factor which affects the detection of the hole boundary signature. Of twenty LASCO profiles examined during the period of 15 August 1996 to 8 September, 1996, only in four was the coronal hole boundary not observed. All four cases for which the coronal hole boundary was not detected involved low-latitude streamers.

The coronal hole boundary has generally been thought to diverge significantly with increasing radial distance (Munro and Jackson 1977, Gosling et al. 1995). This is indeed the general impression one gets from white-light images of the inner corona, such as the Mk III image for 5 September 1996 in Figure 4a. Following this impression, yellow lines that trace the *apparent* coronal hole boundary in both the southern and northern hemispheres have been added to Figure 4a, in contrast with the radial extension of the coronal hole boundaries found in this study and depicted in Figure 4b. The pB profiles of the Mk III coronagraph at altitudes 1.15–1.95 Ro are displayed in Figure 4c. Note that the

vertical scale is logarithmic in order to accommodate the wider range of pB values at the higher altitudes. Here too the vertical red lines identify the radial extension of the coronal hole boundaries. As pointed out earlier, path-integrated density rises by about a factor of two across the coronal hole-streamer boundary nearest the Sun at 1.15 Ro (see for example Figures 1e and 2d). The highest pB values occur where the streamer narrows quickly with increasing heliocentric distance, and reach a level that is at least a factor of ten higher than that in the coronal hole by 1.35 Ro. The blue lines on the pB profiles mark the corresponding locations of the apparent coronal hole boundaries depicted by the yellow lines in Figure 4a, and where the pB values are close to an order of magnitude higher than those in the coronal hole. In comparison, the actual coronal hole boundary which extends radially into interplanetary space, is a weaker feature with only about a factor of two increase in pB.

While pB values in coronal holes are conspicuously low, the azimuthal profiles of pB near the Sun sometimes show considerable variation. Contamination from fore- and background structures enhance the pB values. The Yohkoh soft X-ray images of overlying structures reveal their source. For instance, the Mk III pB measurements on 15 August 1996 indicate that path-integrated density is not constant across the coronal hole at 1.15 Ro (see Figure 2d), but has a minimum at 30° east of north. This is consistent with the Yohkoh soft X-ray image in Figure 2a showing background structures to the west leading to enhanced density there, and a corona free of fore- and background structures in the vicinity of 30° east of north. Moreover, the path-integrated density profiles reflecting coronal density do not change significantly with increasing heliocentric distance. Good examples are the northern polar coronal holes of 5 September 1996 (Figure 3d) and 15 August 1996 (Figure 2d), and the eastern portion of the northern polar coronal hole of 11 August 1997 (Figure 1e). Thus, the coronal hole boundary is not an isolated feature of the corona that extends radially, but appears to be an integral part of the general coronal density profile that is preserved during radial expansion.

Finally, it is interesting to note that the southern polar coronal hole in Figures 1a, 2a, and 3a appears shallow because of the tilt of the Sun. Foreground structures resulting from this tilt may be the reason why the C3 levels of the western portions of the southern polar coronal hole appear high.

3. RAYLIKE STRUCTURES

The images and intensity profiles of the C2 and C3 coronagraphs shown in Figures 1–3 strikingly demonstrate the raylike structures detected by radio occultation measurements. The raylike structures are especially evident near the inner portions of the fields of view of the coronagraphs. As with the Mk III coronagraph, they are not detected at the larger distances because of reduced sensitivity and dynamic range (Brueckner et al. 1995). On the other hand, the superior sensitivity and dynamic range of radio occultation measurements (ranging and Doppler) (Woo 1996a) enables them to detect faint and low-contrast structures even at large distances from the Sun.

Radio occultation measurements show that there are raylike structures smaller than those observed in the LASCO images (Woo et al. 1995, Woo 1996c). The spatial resolutions of C2 and C3 are not necessarily the limiting factor. The 23" spatial resolution of the C2 coronagraph translates to an angular resolution of 0.5° (measured from Sun center) for raylike structures at 3 Ro, while the 112" spatial resolution of the C3 coronagraph to an angular resolution of 1.1° at 6 Ro. The smaller-scale structures that make up the larger plume-like structures are not readily evident in the LASCO images, most likely for the same reason that they are not in ranging measurements of path-integrated density (Woo and Habbal 1997a). They are masked by the larger plume-like structures because the contrast of the smaller rays is only tenths or a few percent (Woo 1996a) compared with the ±10% for the plume-like structures.

As visible in Figures 1–2, raylike structures are present on both sides of the radial extension of the polar coronal hole boundary. The raylike structures in the brighter corona

could not have originated from the polar coronal hole, because the fainter structures from the coronal hole would have been overwhelmed by the brighter corona. Moreover, the dense open raylike structures can sometimes be traced from the quiet Sun to interplanetary space, as is the case of the two structures beyond the boundary of the norther polar coronal hole on the west on 15 August 1996. The approximate locations of the two structures are indicated by the dashed blue lines in Figure 2d.

3. SUMMARY AND CONCLUSIONS

While it has become abundantly clear from a variety of radio occultation measurements that the solar corona is filled with a hierarchy of filamentary or raylike structures (Woo 1996b,c), an obvious validation of these coronal features is to relate them to similar features imaged by white-light coronagraphs. With the Spartan white-light measurements (Fisher and Guhathakurta 1995), this was possible only in the case of coronal streamers (Woo 1996a), because they are composed of the brightest, highest contrast, large-scale (larger than 0.5° in angular size) filamentary structures in the corona. The availability of the LASCO measurements, which afford higher sensitivity and wider dynamic range, has now made it possible to investigate the fainter and lower contrast filamentary structures.

Streamers — characterized by enhancements in path-integrated density of factors ten or more relative to coronal holes — are the brightest features in the solar corona. Their dominance in the corona has given a false impression of diverging coronal holes in white-light pictures. Instead, the boundary of the polar coronal hole — characterized by a latitudinal increase of about a factor of two in path-integrated density from coronal hole to neighboring quiet Sun — extends into interplanetary space approximately radially. The boundary is not evident in all measurements. Detection depends on several factors, including measurement sensitivity, the proximity of the coronal hole boundary to active regions and coronal streamers, and the latitudinal extent of the coronal hole boundaries on

the solar disk. This ledge has been identified in *in situ* plasma density measurements of the solar wind as a halo (Bavassano et al. 1997).

Contamination by fore- and back-ground structures can also cause elevated levels in the white-light density profiles across coronal holes. The Yohkoh soft X-ray measurements identify the source of this contamination. The coronal hole boundary is not the only feature, but appears to be an integral part of the general coronal hole density that extends radially. Thus, in contrast with the profiles of streamers, which are characteristic of a feature that evolves with increasing radial distance, the profiles of coronal holes are preserved during radial expansion.

In the outer corona, where streamers have narrowed to stalks occupying a small volume of interplanetary space (Wang et al. 1997), the corona is dominated by raylike structures as small as a few degrees in angular size. Known as plumes or polar rays in polar coronal hole regions, these raylike structures originate from the quiet Sun as well as coronal hole regions. Smaller-scale structures, which comprise the larger plume-like structures, have been observed in radio occultation measurements but are more difficult to detect in the LASCO white-light pictures, not only because of their smaller size, but also because of their lower contrast. The domination of plume-like structures is also manifested in the spatial distribution of density variations across the raylike structures. The spatial spectrum is inverse power-law, indicating that the density variations decrease with decreasing spatial scale (Woo and Habbal 1997b).

In conclusion, the LASCO observations of raylike structures and the radial extension of the coronal hole boundary provide additional support for the earlier implications from radio occultation measurements — namely that with the exception of the narrowing of streamers into stalks, the coronal density projects itself almost radially from the Sun into the outer corona. These results also reinforce the view that the fast wind originates from both coronal holes and quiet Sun regions (Woo and Habbal 1997a, Habbal et al. 1997).

We thank J.W. Armstrong for many useful discussions, J. Burkepile of HAO for generously providing the Mauna Loa K-coronameter (operated by NCAR/HAO) data, and C. Copeland for skillfully producing the figures. The NSO/Kitt Peak He I λ10830 data used here are produced cooperatively by NSF/NOAO, NASA/GSFC, and NOAA/SEL. We thank the Yohkoh Data Archive Center for the Yohkoh soft X-ray images. This paper describes research carried out at the Jet Propulsion Laboratory, California Institute of Technology, under a contract with the National Aeronautics and Space Administration. Support for S.R. Habbal was provided by NASA grant NAG5-6215. This study was made possible only through the efforts of the entire SOHO LASCO team. Financial support came from NASA and from the Office of Naval Research.

REFERENCES

Bavassano, B., Woo, R., & Bruno, R. 1997, Geophys. Res. Lett., 24, 1655

Bird, M.K. & Edenhofer, P. 1990 in Physics of the Inner Heliosphere: Large-Scale Phenomena, ed. R. Schwenn and E. Marsch (Berlin: Springer) 13

Brueckner, G.E., et al. 1995, Sol. Phys., 162, 357

Fisher, R., & Guhathakurta, M. 1995 ApJ., 447, L139

Fisher, R., Lee, R.H., MacQueen, R.M., & Poland, A.I. 1981, Appl. Opt., 20, 1094

Gosling, J.T., et al. 1995, Geophys. Res. Lett., 22, 3329

Guhathakurta, M. 1989, Ph.D. thesis, U. of Denver

Guhathakurta, M., & Fisher, R. 1995, Geophys. Res. Lett., 22, 1841

Habbal et al. 1997, ApJ., 489, L103

Koutchmy, S. 1977, Sol. Phys., 51, 399

Lallement, R., Holzer, T.E., & Munro, R.H. 1986, J. Geophys. Res., 91, 6751

Munro, R.H., & Jackson, B.V. 1977, ApJ., 213, 874

Newkirk, Jr., G. 1967, Ann. Rev. Astron. Astrophys., 5, 213

Saito, K., Publ. Astron. Soc. Japan, 1965, 17, 1

Tsuneta, S., et al. 1991, Sol. Phys., 136, 37

van de Hulst, H.C. in The Sun, ed. G.P. Kuiper (Chicago: U. Chicago Press) 207

Wang, Y.-M., et al. 1997 ApJ., 485, 875

Woo, R. 1996a, in Proc. Solar Wind Eight, ed. D. Winterhalter, J. Gosling, S.R. Habbal, W. Kurth, & M. Neugebauer (New York: AIP), 38

Woo, R. 1996b, ApJ., 464, L95

Woo, R. 1996c, Nature, 379, 321

Woo, R., & Habbal, S.R. 1997a, Geophys. Res. Lett., 24, 1159

Woo, R., & Habbal, S.R. 1997b, ApJ., 474, L139

Woo, R., Armstrong, J.W., Bird, M.K., & Pätzold, M. 1995b, ApJ., 449, L91

FIGURE CAPTIONS

Figure 1. Observations on 11 August 1997. The straight yellow radial lines superimposed on the images (red lines on the profiles) of the corona indicate the radial extension of the polar coronal hole boundaries. The dashed green line represents the low-latitude extension of the ledge. (a) Combined images of Yohkoh soft X-ray and Mk III Mauna Loa K-coronameter pB. The yellow line on the disk traces the coronal hole boundary as defined by the He I 1083 nm maps of the National Solar Observatory. (b) Combined images of SOHO LASCO C2 intensity and Mauna Loa pB. (c) Image of LASCO C3 intensity. (d) Image of LASCO C3 polarized intesity. (e) Azimuthal pB (top), C2 intensity (middle), and C3 intensity (bottom) profiles as a function of position angle (measured counterclockwise starting from 0° at the north pole).

Figure 2. Observations on 15 August 1996, similar to Figure 1 without a C3 pB image. The dashed blue lines show the approximate locations of two structures originating in the quiet Sun and extending approximately radially outwards from the Sun.

Figure 3. Observations of 5 September 1996, similar to Figure 1 without a C3 pB image.

Figure 4. Same as Figure 3a except that the yellow lines follow the *apparent* boundary of the streamer. (b) Same as (a) except the radial yellow lines superimposed on the corona now indicate the radial extension of the coronal hole boundaries. (c) pB profiles from the Mk III Mauna Loa K-coronameter. The red vertical lines indicate the location of the radial extension of the coronal hole boundary on the pB profiles, while the blue lines mark the locations of the coronal hole boundary corresponding to the yellow contour in (a).

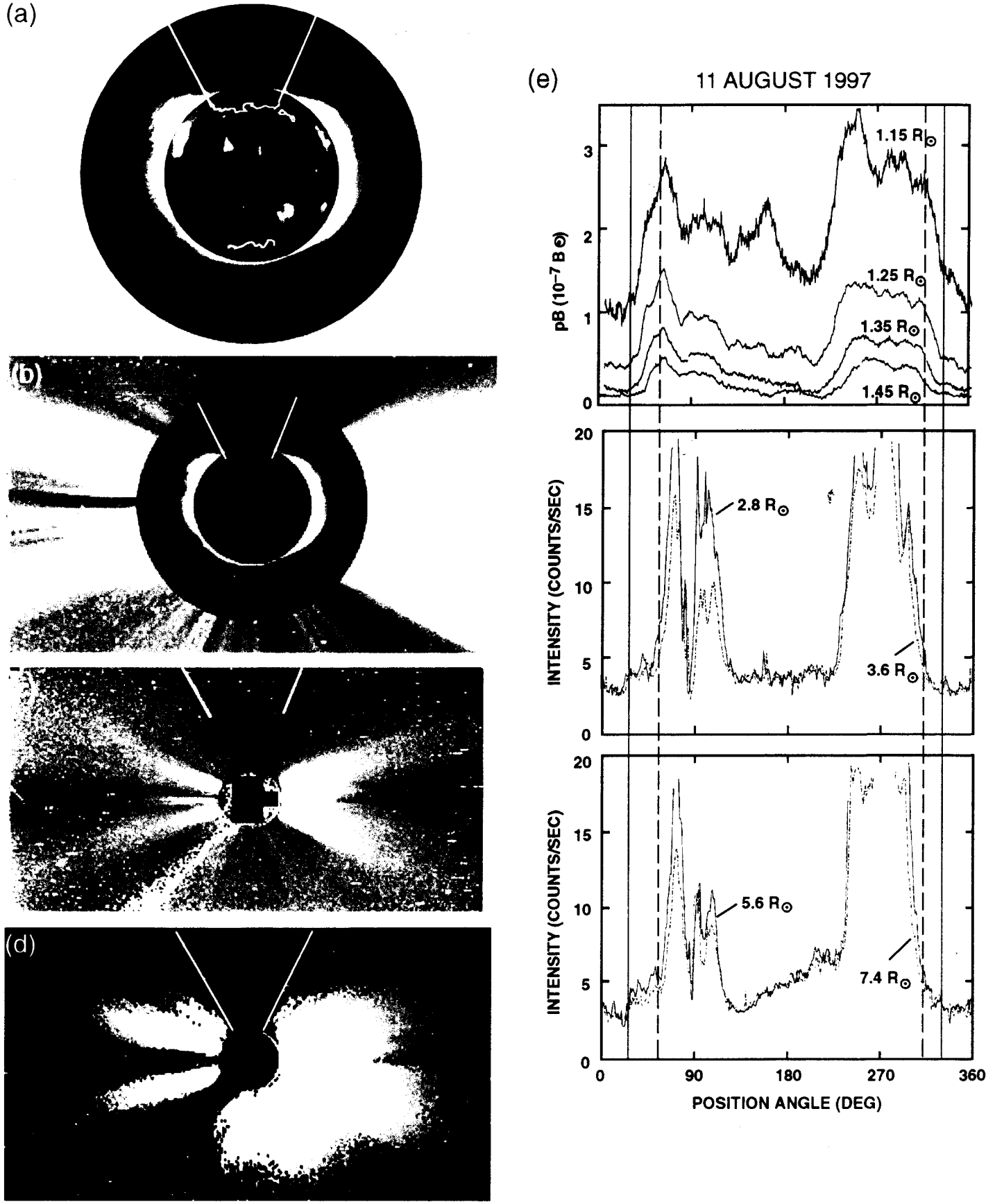
(a)
(b)
(d)
(e)
11 AUGUST 1997
1.15 R⊙
1.25 R⊙
1.35 R⊙
1.45 R⊙
pB (10⁻⁷ B⊙)
2.8 R⊙
3.6 R⊙
INTENSITY (COUNTS/SEC)
5.6 R⊙
7.4 R⊙
INTENSITY (COUNTS/SEC)
0
90
180
270
360
POSITION ANGLE (DEG)

Fig. 1

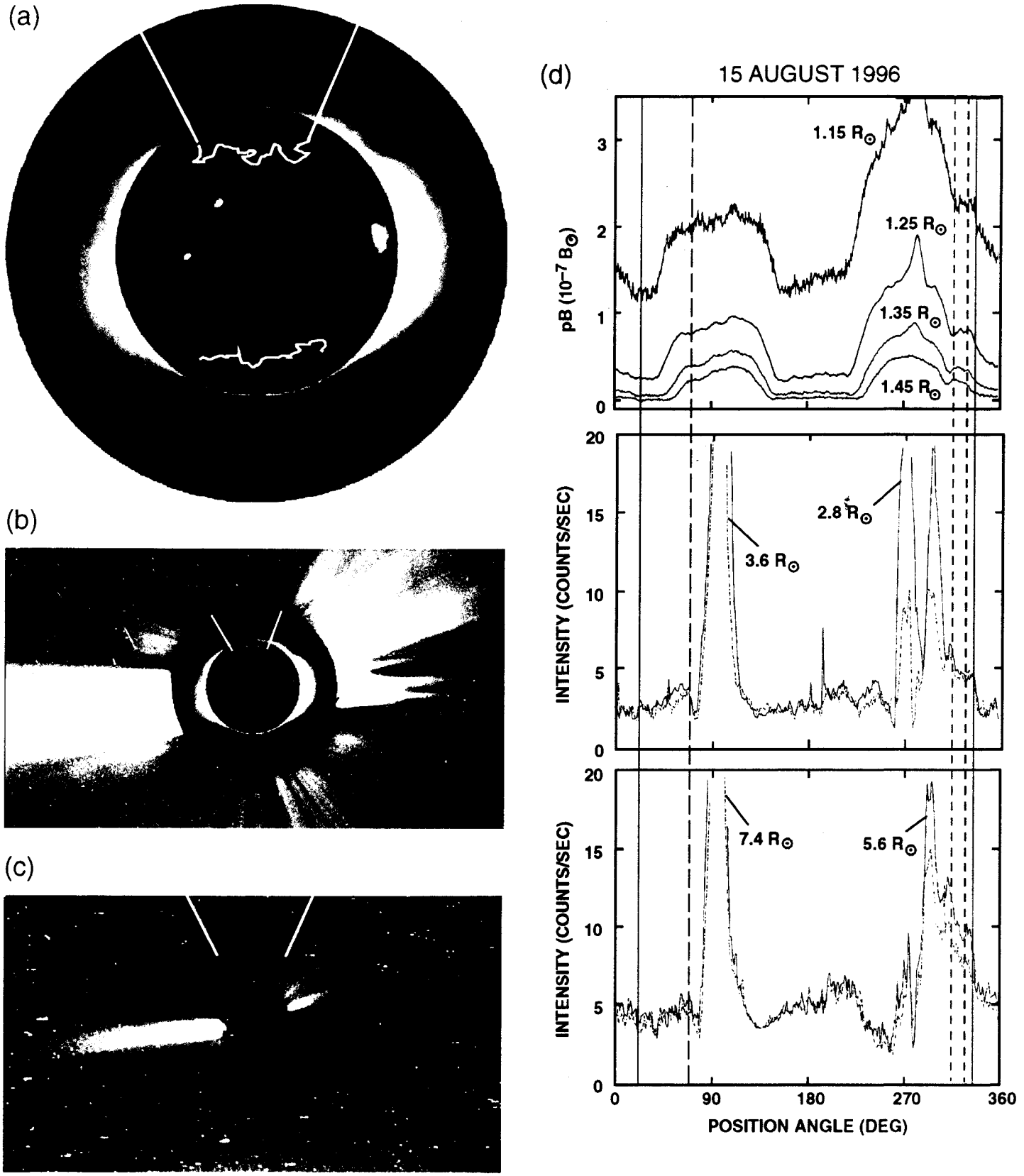
(a)
(b)
(c)
(d)
15 AUGUST 1996
1.15 R⊙
1.25 R⊙
1.35 R⊙
1.45 R⊙
pB (10⁻⁷ B⊙)
2.8 R⊙
3.6 R⊙
INTENSITY (COUNTS/SEC)
7.4 R⊙
5.6 R⊙
INTENSITY (COUNTS/SEC)
0
90
180
270
360
POSITION ANGLE (DEG)

Fig.2

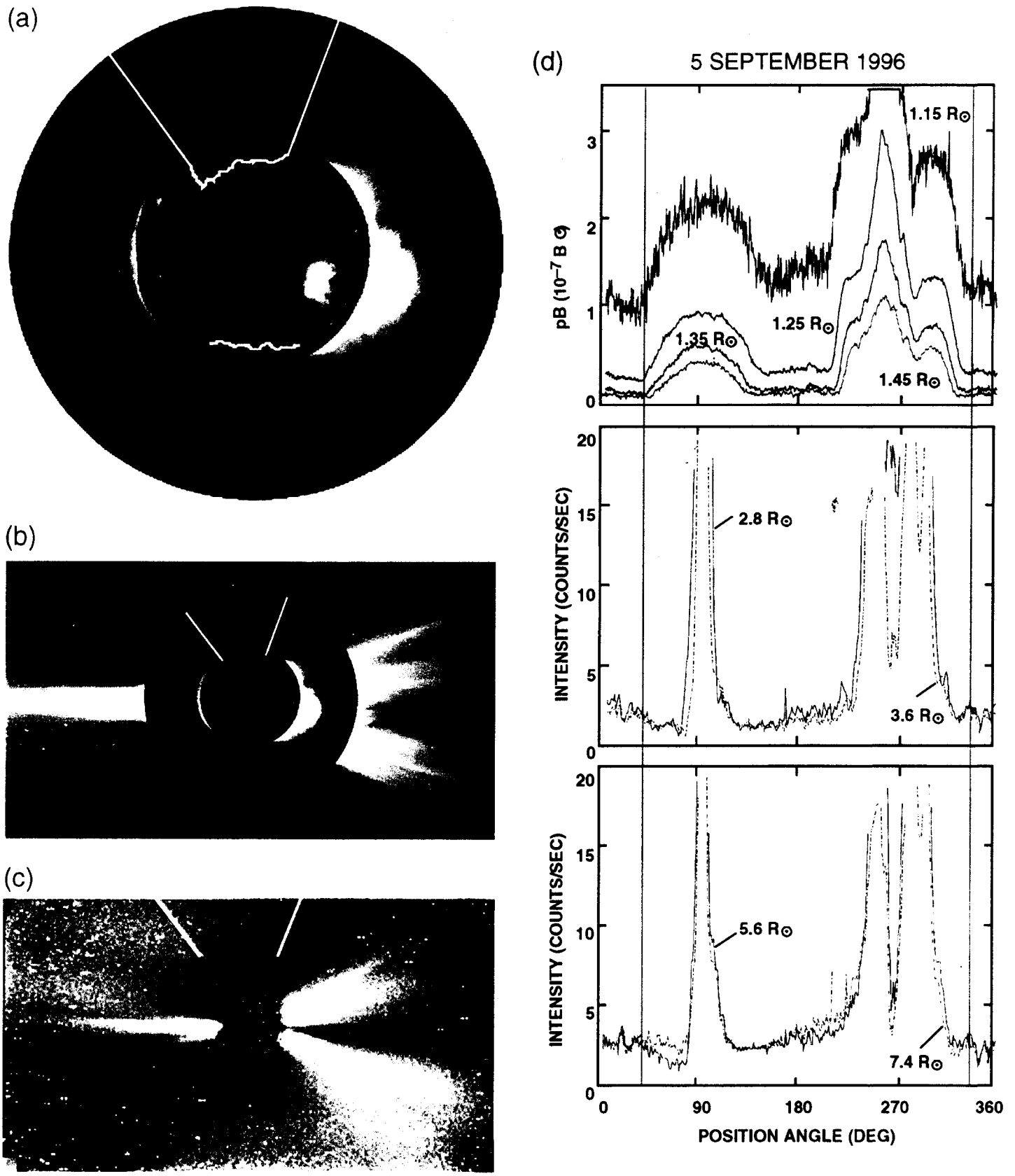
(a)
(b)
(c)
(d)
5 SEPTEMBER 1996
1.15 R⊙
1.25 R⊙
1.35 R⊙
1.45 R⊙
pB (10^{-7} B ⊙)
2.8 R⊙
3.6 R⊙
INTENSITY (COUNTS/SEC)
5.6 R⊙
7.4 R⊙
INTENSITY (COUNTS/SEC)
0
90
180
270
360
POSITION ANGLE (DEG)

Fig. 3

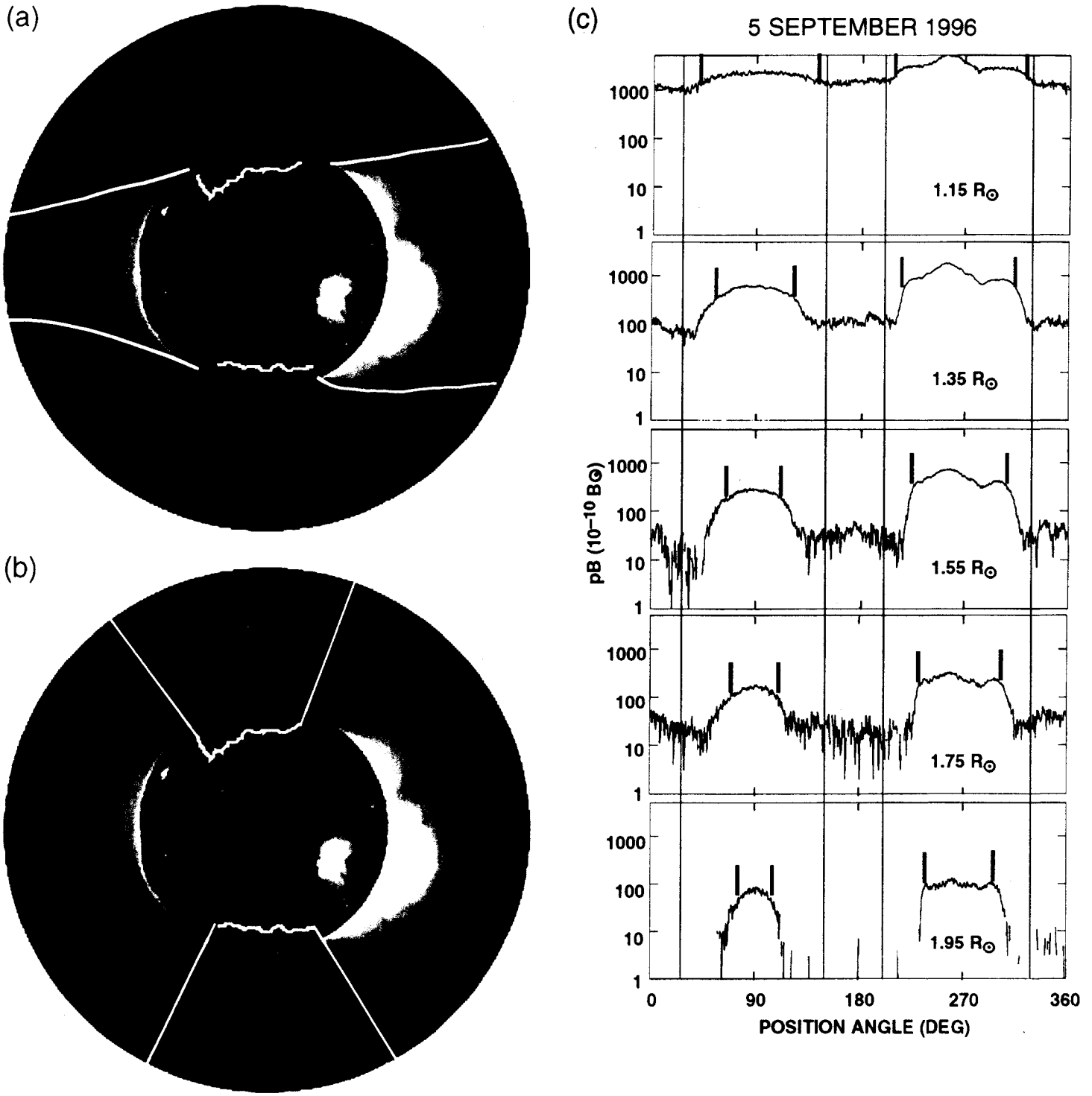
(a)
(b)
(c)
5 SEPTEMBER 1996
1000
100
10
1
1.15 R⊙
1.35 R⊙
1.55 R⊙
1.75 R⊙
1.95 R⊙
pB (10⁻¹⁰ B⊙)
0
90
180
270
360
POSITION ANGLE (DEG)

Fig. 4